## Title

SOME NEW RESULTS IN THE CHARACTERIZATION OF DEFECTS IN PHOSPHOROUS ION-IMPLANTED SILICON



## Authors

Seshan, K.
Washburn, J.

## Publication Date

1974-12-01

Submitted to Radiation Effects

LBL-2776
Preprint

# SOME NEW RESULTS IN THE CHARACTERIZATION OF DEFECTS IN PHOSPHOROUS ION-IMPLANTED SILICON

K. Seshan and J. Washburn



December, 1974

Prepared for the U. S. Atomic Energy Commission
under Contract W-7405-ENG-48



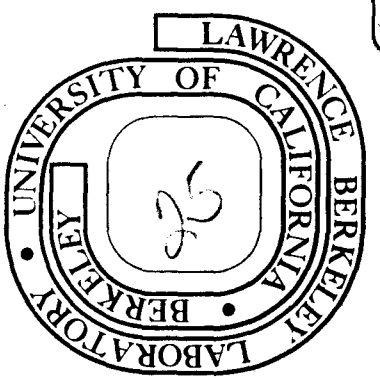

## DISCLAIMER

# SOME NEW RESULTS IN THE CHARACTERIZATION OF DEFECTS IN PHOSPHOROUS ION-IMPLANTED SILICON

K. Seshan and J. Washburn

Department of Materials Science and Engineering,
College of Engineering and Inorganic Materials Research Division
Lawrence Berkeley Laboratory, University of California
Berkeley, California 94720

## ABSTRACT

Defects in annealed $P^+$ ion-implanted silicon (p type), implanted to below the critical dose to form a continuous "amorphous" layer, were found to be faulted hexagonal Frank loops (~$10^{16}/cm^3$, 200Å in diameter) on the four {111} planes. A few unfaulted loops and linear defects (~$10^{13}/cm^3$, ~800Å in length) along the <110> directions were also present. The loops showed contrast effects indicative of solute segregation within the loop. The displacement vectors are then of the type $\frac{a}{x}$ [111] with x slightly greater than three. The loops were all interstitial suggesting that they form from the conversion and growth of small interstitial clusters formed during implantation. Segregation of dopants to these interstitial clusters could account for the poor electrical activity of phosphorous in foils implanted to below the critical dose and annealed in the 500-700° range. Studies of n type (P and Sb doped) foils show that defect morphology varies with foil type (n- or p-) and dopant species present prior to implantation. Evidence that the linear defects are interstitial type, that they anneal from the end near the free surface and that boron is necessary for their formation is also presented.

## INTRODUCTION

The recovery of electrical activity of $P^+$ implants in silicon depends critically on the dose. It is known that for implants just below the "critical dose", i.e. before the formation of a continuous "amorphous" layer, a high proportion of the implanted ions (70% after a 600°C anneal, ~20% after a~800°C anneal) are still inactive.(1)

Precipitation at or near the dislocation loops formed on annealing has been suggested.(2) However, the exact nature of the process is not clear. It has been proposed that the impurities are attracted to the dislocation core. However, this attraction is weak for phosphorous.(3)

The present experiments were undertaken to characterize the type of loops present and to attempt to obtain evidence for segregation of phosphorous atoms to the loops.

Differing accounts of defect morphology in $P^+$ implants now exist. Circular perfect loops in the foil plane have been reported.(2,4) Other studies show mostly hexagonal Frank loops.(5,5a) One author(6) denies the presence of linear defects in $P^+$ implants, while others report their presence.(4,7,8)

The present experiments were carried out to explain the above differences and to test the hypothesis that loop type and the presence of linear defects depend on foil type and on the dopant elements present prior to implantation.

## EXPERIMENTAL

Silicon foils (p-type boron doped 0.2 - 8Ωcm, and n-type phosphorous or antimony doped ~1Ωcm) were implanted 8° off <111> to a dose of $2 \times 10^{14}$

ions/cm$^2$ with 100 keV $P^+$ ions at room temperature with currents of ~1μA/cm$^2$. One p type foil was implanted with $Si^+$ ions to a dose of $2 \times 10^{14}$ ions/cm$^2$. Samples for electron microscopy were annealed in the range 600°C - 800°C in extra pure helium, chemically thinned from the non-implanted side and examined at 100 keV in a Philips 301 and a Hitachi Hu 125 electron microscope.

RESULTS

In Section A the loops lying in the foil plane are analyzed and shown to be interstitial type (Fig. 1). Figures 1d and 3a-e show weak-beam images of these defects. Several loops (e.g. β and γ in Fig. 1d; A in Fig. 3e) appear hexagonal with fringes indicating that they are faulted and lie on planes inclined to the (111) foil surface. In Section B, their inclination is calculated using the fringe spacing variation (Fig. 3a-e). In Section C, the results of changing substrate dopant and the effects of segregation are discussed. Finally, Section D is on the nature and behaviour of the linear defects.

## SECTION A

### Analysis of Loops Lying in the Plane of the Foil

Figure 1a shows the conventional bright field image at the (111) pole with $g = 02\bar{2}$. Loops in the foil plane (e.g. δ in Fig. 1a and 3b) appear in residual contrast ($g.b = 0$). In Fig. 1b and c the same area is imaged at the [211] pole with ±g ($g = [11\bar{1}]$). Loops in the foil plane now appear as grey hexagonal discs with edges along <110> directions (Fig. 1b or A in Fig. 3e). They show strong "inside" contrast (Fig. 1b).

Fig. 2a shows the crystal orientation that was determined from the Kikuchi pattern and was used for analysis of loop type. Vectors for the

foil normal $\hat{n}$, the operating reflection $\hat{g}$ and the condition for 's' (the deviation parameter)[9a] being positive are shown in Fig. 2b. In terms of the FS/RH convention (Fig. 2c) only interstitial loops in the foil plane satisfy the condition $(g.R)s>0$ ($g = 1\bar{1}\bar{1}$ $R = \bar{1}\bar{1}\bar{1}$, $s>0$) This gives "inside" images [9b] as observed in Fig. 1b. The analysis in terms of the rotation of planes gives the same result (Fig. 2d) as do the weak-beam images (1d). It is concluded that the loops in the plane of the foil are interstitial type.

A dislocation reaction consistent with this conclusion is seen in Fig. 1b and d at E. Here a loop on the inclined plane has grown into contact with a loop in the plane of the foil. The two meet at 120° and the two Frank dislocations have combined to form a stair-rod dislocation. Therefore, the defects on the two planes must have been of the same type i.e. both were interstitial type. Loops on the inclined planes have previously been shown to be interstitial.[5,5a] This may also be deduced using Fig. 2b.

It has been suggested[10] that loops in the foil plane are vacancy type. If this were so or if loops in the foil plane had been found to lie at a different depth it would suggest an effect of internal stress (caused by the swelling of the amorphous regions) on the nucleation or growth of loops. Fig. 5 shows the result of stereoscopic depth distribution measurements. Loops in the foil plane ($\delta$) were found to be dispersed uniformly with those on the inclined planes within the same depth range. Therefore, no effect of internal stress on nucleation or growth was detected in these foils which were damaged to less than the critical dose.

## SECTION B

### Determination of Loop Habit Planes

The spacing of the fringes in defects like A (Fig. 3a-e) depend only on the effective extinction distance $\xi g^w$ and the inclination $\theta$ of the fault habit plane to the foil plane. For the kinematical condition (large s) under thich these weak beam images were obtained the fringe spacing is $\xi g^w \cot\theta$ (9c). Assuming that the loops lie on an inclined {111} plane, $\theta$ is 70°.

Table 1, column 1 shows the weak-beam reflecting conditions corresponding to Fig. 3a, c and d. The calculated values of the deviation parameter Sg and the dimensionless deviation w, which equals Sg times the extinction distance $\xi_g^\circ$, are shown in column 3 and 4 respectively. This was used to find the effective extinction distance $\xi_g^w$ in column 5 using the formula $\xi_g^w = \xi_g^\circ / \sqrt{1+w^2}$, where $\xi_g^\circ$ for silicon g = 220 is 757Å. Fringe spacing was calculated from the formula $\xi_g^w \cot 70°$ and is shown in column 6. These agree within the experimental error (±0.1mm = 10Å) with the spacing measured on the plate and shown in column 7. This validates the assumption that the loops lie on {111} planes.

Table 1

Fringe spacing as measured on the electron micrographs are shown in column 7. These agree within experimental error (±10Å) with calculated values shown in column 6. The calculations assumed that the loops lie on an inclined {111} plane.

| 1 | 2 | 3 | 4 | 5 | 6 | 7 |
|---|---|---|---|---|---|---|
| Weak-beam reflecting condition | Fig. | $(Sg)\mathring{A}^{-1}$ | w | $\xi_g^w$ Å | Calculated spacing Å | Measured spacing Å |
| g/2g | 3a | $5.05 \times 10^{-3}$ | 3.83 | 190 | 69 | 70.5 |
| g/3g | 3c | $1.14 \times 10^{-3}$ | 8.65 | 87 | 32 | 35 |
| g/4g | 3d | $2.02 \times 10^{-2}$ | 15.30 | 49 | 18 | 20 |

The edges of the loops lying in the foil plane (Fig. 1b) and those inclined to the foil plane (Fig. 3e at A) lie accurately along <110> or projected <110> directions. Since only {111} planes contain three coplanar <110> directions, this is further evidence that the defects lie on (111) planes.

Finally, four sets of loops were observed as would be expected if the habit planes are {111} .

## SECTION C

### On Loop Morphology

The morphology of the defects for p-type foils in the resistivity range 0.2-8Ωcm was similar to that shown in Fig. 1 and 3. They were mostly faulted hexagonal loops on the four {111} planes, present in concentrations between $10^{13}$-$10^{15}/cm^3$ and were between 200-300Å in diameter. In addition, there were a few circular unfaulted loops whose interiors appreared much darker than adjacent areas, e.g. Fig. 1d at A, B and D in the weak-beam positive print.

The hexagonal Frank loops in the foil plane showed similar contrast. In inside contrast they appeared as black hexagonal discs (Fig. 1b); in outside contrast they were faint and could hardly be seen (Fig. 1c). Weak-beam images also showed this trend. This behaviour is not affected by small changes in 's' and depends only on the sign of (g.b)s. The loops are distributed at various depths within ±1500Å (Fig. 4). Nevertheless, all the loops still show the same effect. Therefore, this is not a depth effect.

It is suggested that this contrast effect in the faulted loops may be a structure factor contrast arising from the adsorption of dopant on the stacking fault. The contrast effect in the perfect loops could result if small displacements normal to the loop plane still remain after unfaulting; i.e. the burgers vector of the unfaulted loop is still not quite a lattice vector.

For $P^+$ ions in these foils implanted to a dose less than the critical dose and annealed to about 800°C up to 20% of the dopant atoms are still inactive.[1] It is possible that these $10^{17}$ atoms/cm$^3$ (corresponding to about 10% of the atoms forming the loops) segregate on the stacking fault within the Frank loop during growth and remain even if the fault has been removed by the nucleation of a Shockley partial. Such a segregation would change the displacement vector of the faulted loop to $\frac{a}{x}$ [111] with x slightly greater than three and those of the perfect loops to $\frac{a}{2}[110] - \frac{a}{y}[111]$.

A different loop morphology was observed in n-type phosphorous doped and antimony doped silicon, for the same dose and annealing treatment as the p-type samples described above. In the phosphorous

doped foils, for both Czochralski grown(Fig. 5a)and vacuum float zoned 'lopex' silicon(Fig. 5b) the loops tended to be more circular. The change in oxygen concentration seemed to have little effect. In the antimony doped foils irregular hexagons were seen,(Fig. 5c,d) In weak-beam images near the g/3g Bragg condition ($g = \bar{2}20$) these loops had no fringe contrast suggesting that they are perfect loops. However, they did exhibit the unusual contrast effects for + and -g, indicative of solute segregation within the loop (e.g. Fig. 5c and d at A).

The shape of the loops could be affected by whether they were growing or shrinking at the end of the final heat treatment. The former tend to be hexagonal, the latter circular assuming that jog nucleation is an important step.[11] Since the dose of $P^+$ ions and the annealing treatment of the n-type and p-type foils were the same the loops are expected to be in the same growth stage. The differences in loop morphology are presumably due to the presence of the different dopants, phosphorous or antimony, present prior to implantation.

The change in loop morphology with prior dopant species suggests that there is an effect of dopant elements on loop nucleation or on unfaulting. This could account for some of the differing morphologies reported in the literature.[2,4-8].

## SECTION D

### On the Presence of Linear Defects

In p-type (boron doped) foils implanted with $P^+$ or $Si^+$ ions linear defects (~8000Å long) in concentrations of about $10^{12}$-$10^{13}/cm^2$ were seen. (This estimate may be low as their images are depth dependent[12] and not all of them are seen). They were absent in the n-type (p-doped

or Sb-doped) foils, (Fig. 5). Since rods were only seen in foils where boron was present (p-type boron doped silicon or $B^+$ implanted silicon) the presence of boron is apparently essential for the rods to form.

Fig. 1 shows that there are few interactions between the linear rods and the loops suggesting that they deplete the same species during growth and so tend to avoid each other. This deduction that the rods are interstitial because the loops are interstitial is consistent with the contrast analysis showing that the rods are extrinsic.[8] Stereo microscopy indicates that the rods along the inclined <110> directions (AD, BD etc., Fig. 13) are much longer (~1μ) than those in the foil plane (~6000-8000Å). The inclined rods extend from the plane of the loops towards the implanted surface. During anneal a great majority of these rods simply shrink from the end but a few grow wider to become loop like. The inclined rods shrink most rapidly from the end nearer to the implanted surface probably by the motion of vacancies from the surface.

One study[6a] reported that linear defects were not present in $P^+$ ion implanted p-type silicon. Another[4] reported that they were present only in hot implants. Linear defects were always found in this study of room temperature implants at subcritical dose;[7] recently similar results have been obtained elsewhere.[8] Experiments in progress indicate that sample heating during implantation may determine whether rods are formed or not.

A catalogue of defects observed, their probable origin and their contrast properties are given in Table II.

## CONCLUSIONS

In phosphorous implanted and annealed p-type (B-doped) silicon foils, loops lying in the (111) foil plane were found to be interstitial as are those on the inclined (111) planes. A majority of the loops were hexagonal in shape, faulted and lay on {111} planes. The displacement vectors of the loops were of the type $\frac{a}{x}[111]$ with x probably slightly greater than three because of absorption of impurity on the stacking fault. The observed interstitial Frank loops on the four {111} planes are probably formed from the break-up of small interstitial clusters formed either during irradiation or during the very early stages of annealing (100-300°C).

The defect morphology resulting from phosphorous implants into n-type, phosphorous or antimony doped samples were different from each other and different from that obtained from p-type foils. This effect of dopants which are initially present, could account for the differing descriptions of loop morphology present in the literature.[2,4-8]

Contrast effects indicate that dopant atoms segregate inside the perfect loops as well as on the stacking faults within the faulted loops. This suggests that the perfect loops were originally faulted and that the segregation remains after unfaulting. This accumulation of dopants to interstitial loops could account for the low phosphorous activity in foils damaged below the critical dose.

Boron has been found to be essential for the formation of linear rod like defects. They are extrinsic in nature and the majority shrink from the ends in the 700°C temperature range. A few grow wider to become loop like.

ACKNOWLEDGMENTS

We are grateful to Dr. V.G.K. Reddi of Fairchild R & D Division, who has provided us with the implanted wafer and to Dr. M.J. Goringe and Professor G. Thomas for numerous helpful discussions. The work was supported by the US AEC through the Lawrence Berkeley Laboratory.

## A Catagogue of Defects - Table II

| Type and example | Contrast features | Physical Characteristics |
|---|---|---|
| Faulted loops on the four 111 planes, e.g. α, β, γ δ in fig. 1a-e.*<br><br>Origin: Clustering of interstitials and the break up of such clusters during annealing. | g = $0\bar{2}2$. Fig. 1a. Only β, γ are seen.<br>: δ loops appear by residual contrast i.e. line of no contrast perpendicular to $\hat{g}$.<br>: loops on α absent: $\hat{g}.\hat{b}_{\alpha} = 0$.<br><br>g = $1\bar{1}\bar{1}$ at 211 pole<br>: α loops are seen edge on (Fig. 1b,d) in strong contrast as $\hat{g}$ and $\hat{b}$ are parallel.<br>: δ loops show strong inside contrast +g and weak outside -g. This is independent of "s". Fig. 1b and Fig. 1c. | Hexagonal, faulted with sides along 110 directions (See loop in Fig. 1b in foil plane and loop A Fig. 3e on an inclined plane).<br><br>There is indication that dopants are segregated on the stacking fault and the displacements are of the type $\frac{a}{x}$ <111> , x>3.<br>Population: numerous for phosphorous ions implanted into p (boron-doped) silicon.<br>Type: Interstitial on all four planes. |
| Unfaulted loops, e.g. A,B,C,D. Fig. 1b.<br><br>Origin: Unfaulting of faulted hexagonal loops and the subsequent rotation off 111 planes or nucleation of perfect loops caused by the presence of dopant elements. | Contrast goes from weak to strong as the operating reflection changed from +g to -g. Indicates precipation of dopants within loop. | Displacements:<br><br>$\frac{a}{2}$<110> -a/y<111><br><br>due to precipitation.<br>Population: very few. However, their numbers are increased with impurity, for Phosphorous ions implanted into n-type (Phosphorous doped or Antimony doped) silicon.<br><br>Loops with habit planes {110} (edge orientation) as well as those rotated off {111} are seen. |

Table II (Con't)

| Type and example | Contrast features | Physical characteristics |
|---|---|---|
| Linear rods AB,AC,CB lying along the three <110>directions in the foil plane and CD,BD,AD along the three <110> directions inclined to the foil plane. Fig. 1b*. | Inclined rods show dotted contrast e.g. DC,DB,DA in Fig. 1d. Behave like dipoles, give inside and outside contrast. | Displacements: $\frac{a}{x}$ <100> ; interstitial lying on {100}. (8a) |
| Form only when boron is present | Contrast and visibility of these defects are very sensitive to position of defect in foil and effective foil thickness. | Rods and loops do not interact. They avoid each other possibly because they compete for the same point defect. Work in progress indicates that the inclined rods are much longer than those in the foil plane. They start at the level of the horizontal rods and extend towards the implanted surface. They anneal from the end near the implanted surface. |

* The lettering used in Fig. 1a, b, and d are consistent with the Thomson tetrahedron drawn on these figures.

REFERENCES

1. B. L. Crowder, and F. F. Morehead Jr., Applied Phys Lett., 14:10, 313 (1969).

2. S. M. Davidson and G. R. Booker, Radiation Effects, 6, 33 (1970).

3. J. F. Gibbons, Radiation Effects, 6, 313 (1970).

4. M. Tamura, I. Ikeda, and N. Yoshihihro, Japan Society of Applied Physics, 40, 9 (1971).

5. M. L. Jenkins, D.J.H. Cockayne, and M. J. Whelan, Journal of Microscopy, 98, 155 (1973).

5A. K. Seshan and J. Washburn, Phys. Stat. Sol. (In Press).

6. R. W. Bicknell and R. M. Allen, Radiation Effects, 6, 45 (1970).

7. K. Seshan and J. Washburn, Radiation Effects, 14, 257 (1972).

8. P. K. Madden, PhD Thesis, Univ. of Oxford (1973).

8A. P. K. Madden, S. M. Davidson, Radiation Effects, 14, 271 (1972).

9A. P. B. Hirsch, A. Howie, R. B. Nicholson, D. W. Pashley, M. J. Whelan, Transmission Electron Microscopy of Thin Crystals, Butterworths, London (1965) p. 164.

B. Ibid, p. 266.

C. Ibid, p. 341.

10. R. W. Bicknell, PhD Thesis, Univ. of London. Phil. Mag., 26, 273 (1972).

11. J. Friedel, Dislocations, Pergamon Press Ltd.,(1964) p. 125.

12. L. J. Chen, K. Seshan, and G. Thomas Lawrence Berkeley Laboratory Report # 1164 (1974), Phys. Stat. Sol. (In Press).

13. P. M. Kelley and R. H. Blake, Phil. Mag., 28, 475 (1973).

FIGURE CAPTIONS

Fig. 1. (a) shows the image of a (111) foil at the [111] pole using a $02\bar{2}$ reflection; loops in the foil plane, e.g. $\delta$ , appear by residual (g.R = 0) contrast.

(b) shows the same area at the [211] pole with g = $1\bar{1}\bar{1}$. Loops in the foil plane appear by diffraction contrast. They show strong inside contrast, lie on the (111) foil plane and have straight edges along 110 directions.

(c) shows the image at the [211] pole with g = $\bar{1}11$. The loops in the foil plane now show weak outside contrast. In Fig. 1b and d the tetrahedron of 111 planes is drawn and the linear defects along the six <110> directions identified.

(d) shows the weak-beam image of the same area at the [211] pole. The $\delta$ loops show uniform white contrast confirming that they lie parallel to the foil surface. Loops on the $\alpha$(BCD) plane appear edge on. Perfect loops marked A,B,C show dark interiors evidencing some form of precipitation inside the loops. At E a loop on the foil plane has reacted with one on an inclined plane. Hence these loops are both interstitial.

Fig. 2. (a) shows the position of the experimentally observed poles and the correct orientation of the crystal as seen in Fig. 1a. (b) shows the crystal rotated to the [211] pole. This condition corresponds to images in Fig. 1b,c and d. The top surface of the crystal is assumed fixed and the images are obtained at g (s>0) i.e., the reciprocal lattice point in inside the Ewald sphere. (c) shows the formal FS/RH analysis. The observed

images require that $g.R>0$. Only interstitial loops in the foil plane satisfy this condition.

(d) shows the analysis repeated in terms of the rotation of planes. This procedure also gives the same result that the loops in the plane of the foil are interstitial.

Fig. 3a-e Shows weak beam images with conditions g/2g (imaging g with 2g satisfied) to g/4g. Notice the increase in the number of fringes in defect A going from two in Fig. 3a to about six in Fig. 3e. The fringe spacing decreases as the deviation parameter "s" increases from $5x10^{-3}$ $A^{-1}$ in fig. 3a to $2.2x10^{-2}$ $A^{-1}$ in fig. 3e. The spacing of these fringes can be used to accurately calculate the inclination of the defect such as A. It is proved (see text) that A is an hexagonal loop lying on an inclined {111} plane. Notice also that A and B have been cut by the foil surface.

Fig. 4. Shows the distribution of loops in the foil plane $\delta$ and those on inclined planes $\alpha$, $\beta$, and $\gamma$. The $\delta$ loops are distributed uniformly and show no preferential locations.

Fig. 5. Phosphorous implants ( $2 \times 10^{14}$ ions/$cm^2$) into:

(a) n (phosphorous doped), Czochralski grown ~1$\Omega$cm Si; symmetric weak-beam bright field (SWBBF) image[16];

(b) n (phosphorous doped) Si, ~$\Omega$1cm, vacuum float zoned "lopex" Si SWWB image;

(c) n (antimony doped) Si, weak-beam images in $\pm$g.

The foils were all heat treated 750 - 800°C for 1/2 hour. Notice the increase in the fraction of almost circular perfect loops over the p type foils (Fig. 1) and the absence of linear defects. In (c) and (d) notice how the large loops show very dark inside contrast (c) and weak outside contrast (d) e.g. at A. This is interpreted as evidence of dopant segregation to the stacking fault before the loop unfaulted.

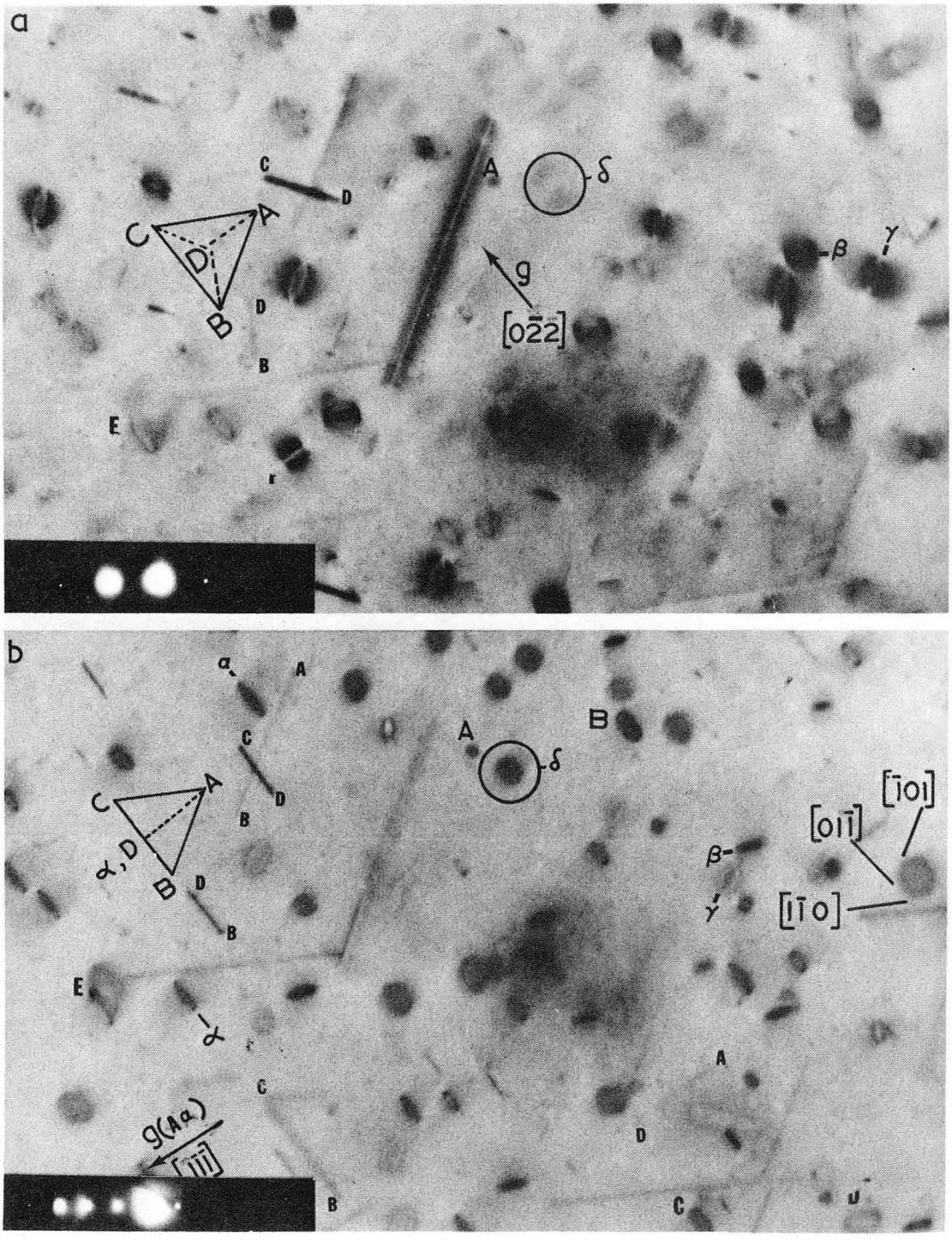


XBB 747-4423

Fig. 1

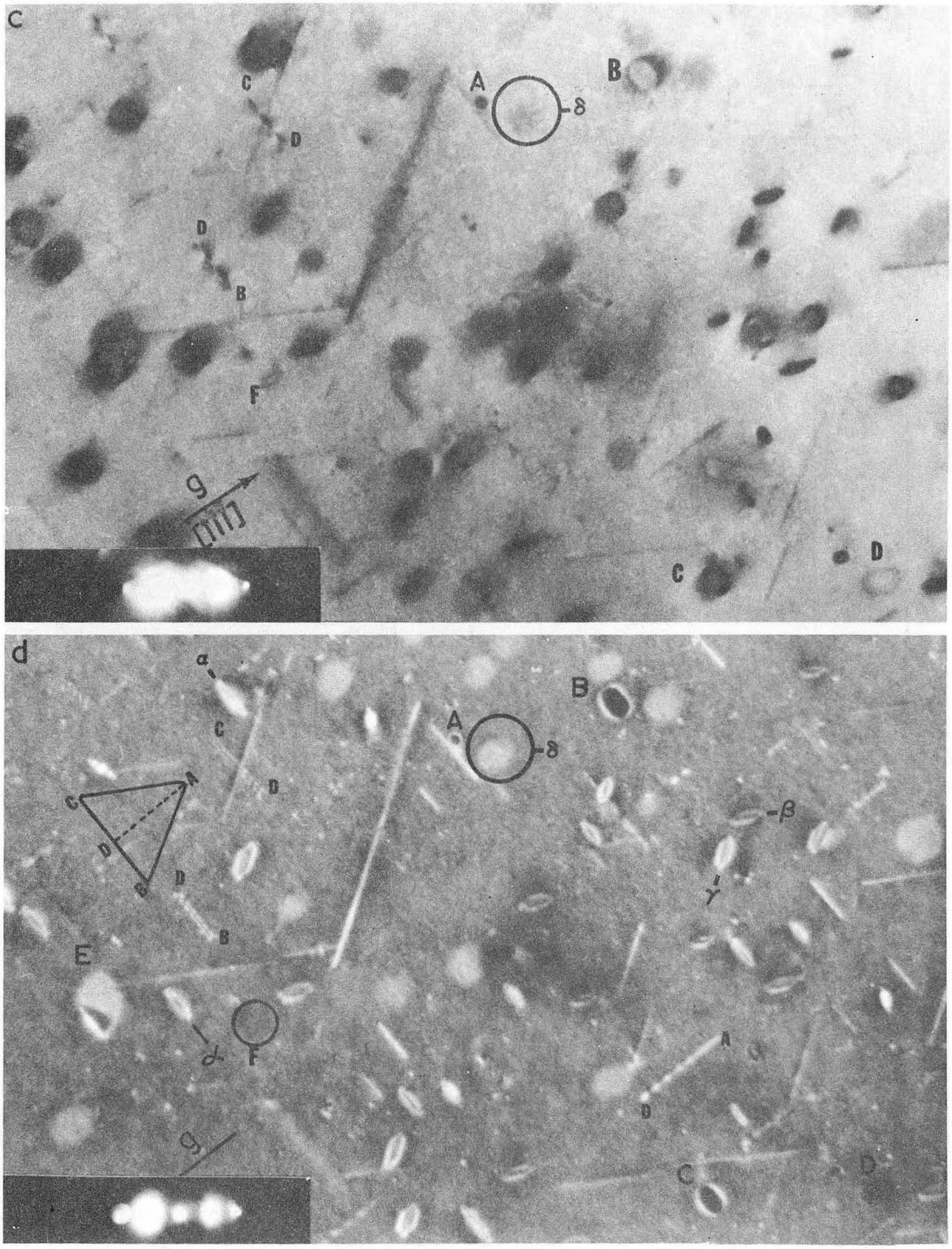


XBB 747-4424

Fig. 1 continued.

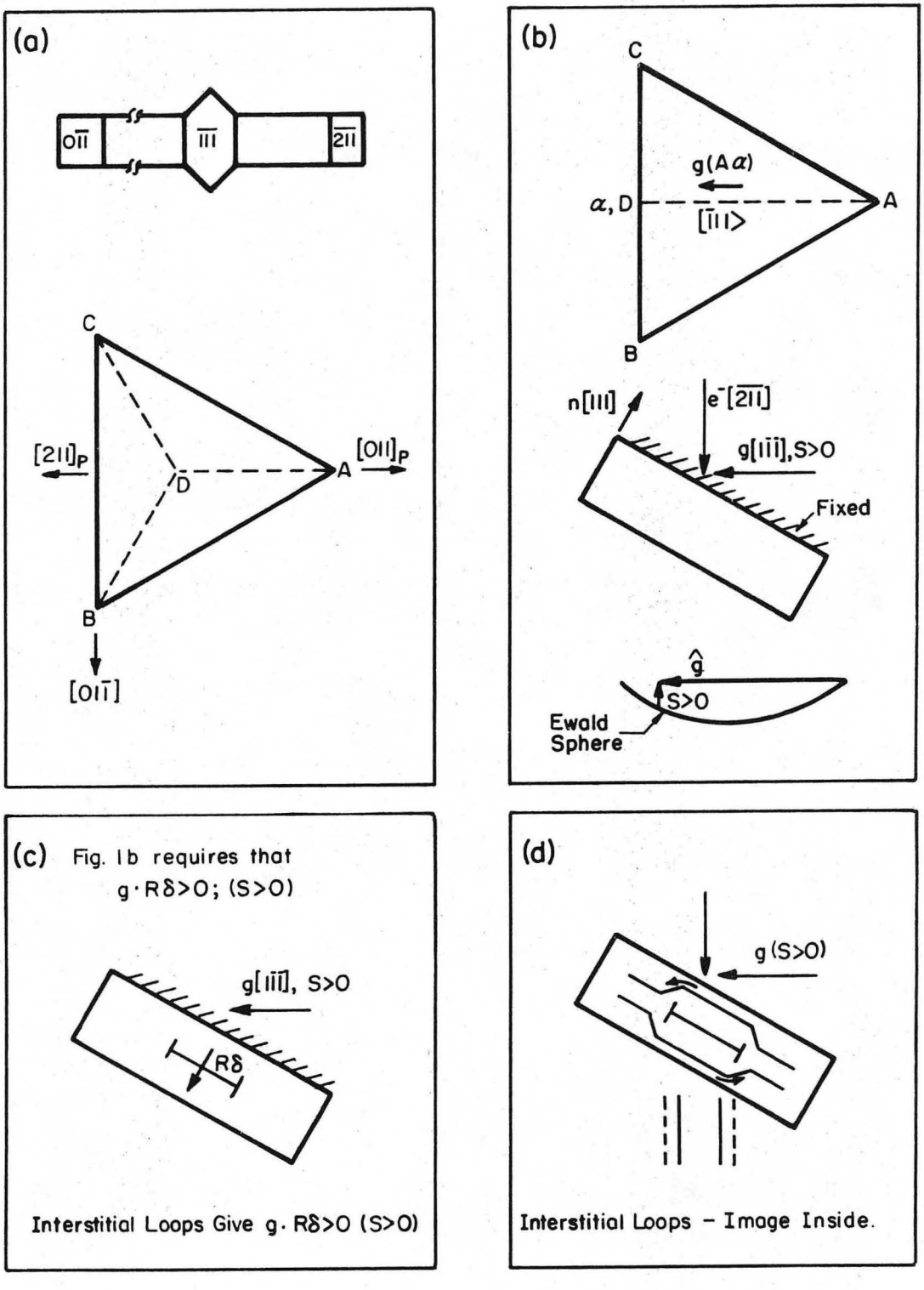


XBL 745-6413

Fig. 2

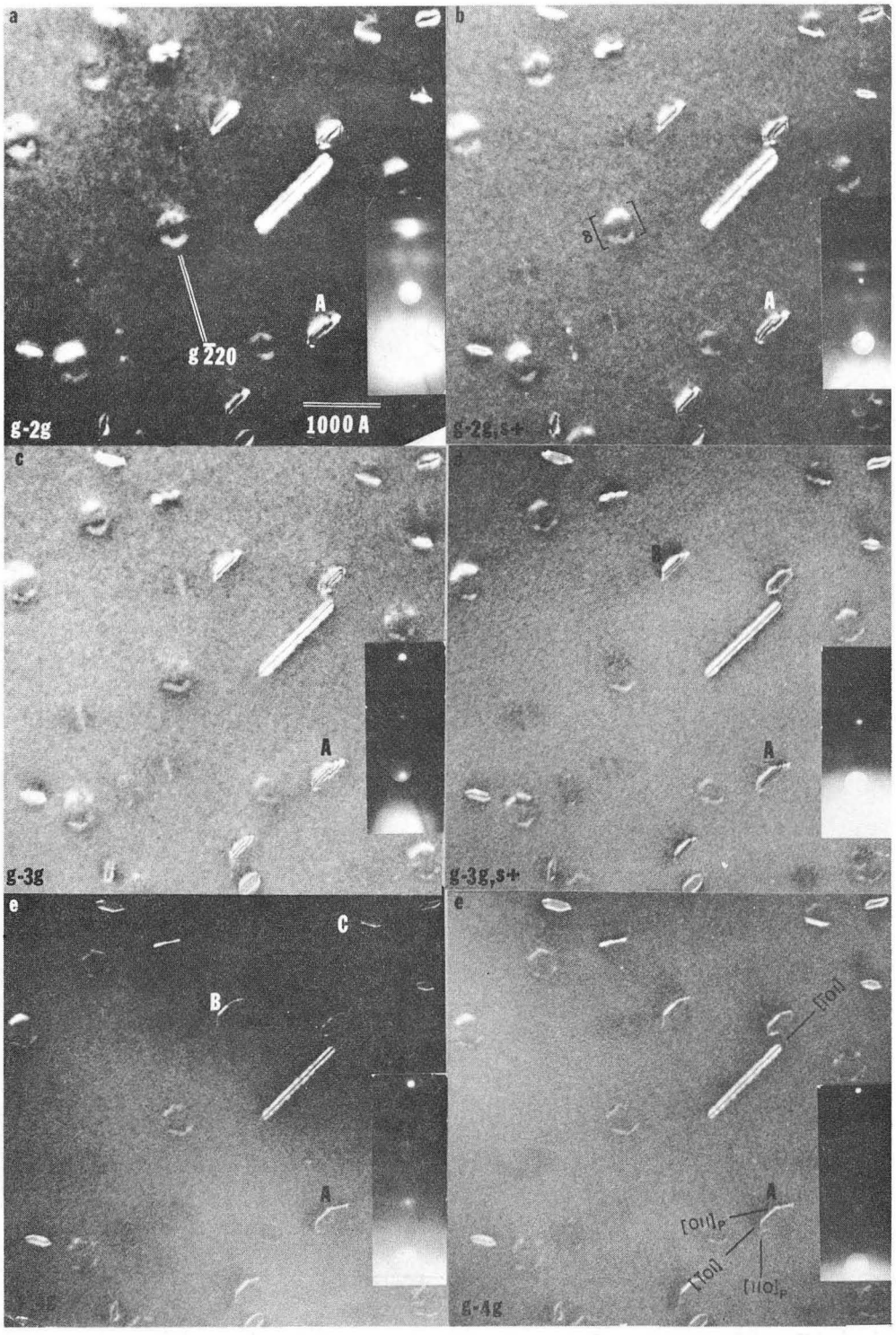


XBB 745-3357

Fig. 3

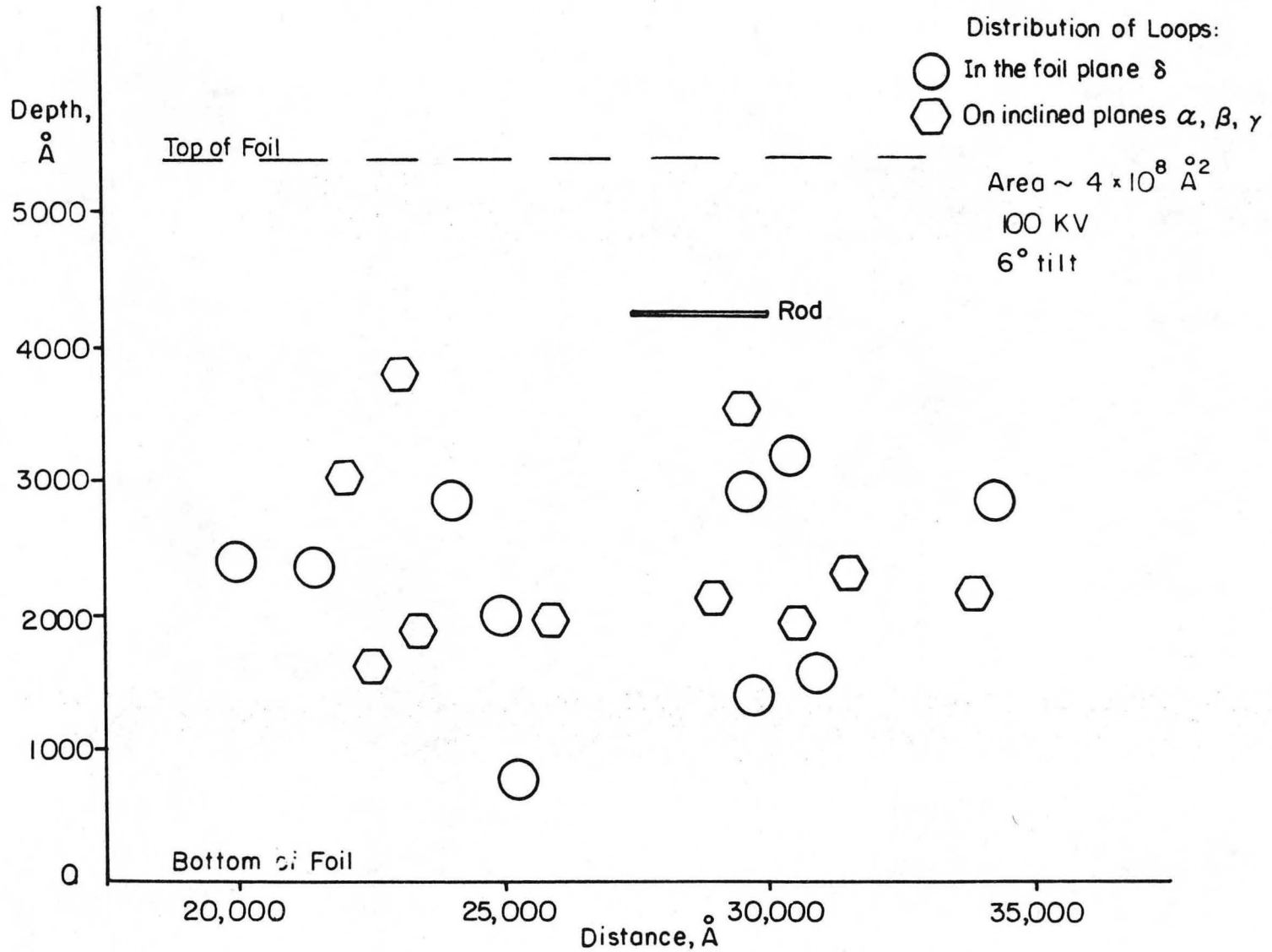
Distribution of Loops:
In the foil plane δ
On inclined planes α, β, γ
Area ~ 4 × 10^8 Å^2
100 KV
6° tilt
Depth, Å
Top of Foil
Rod
5000
4000
3000
2000
1000
0
Bottom of Foil
20,000
25,000
30,000
35,000
Distance, Å
XBL747-6673

Fig. 4

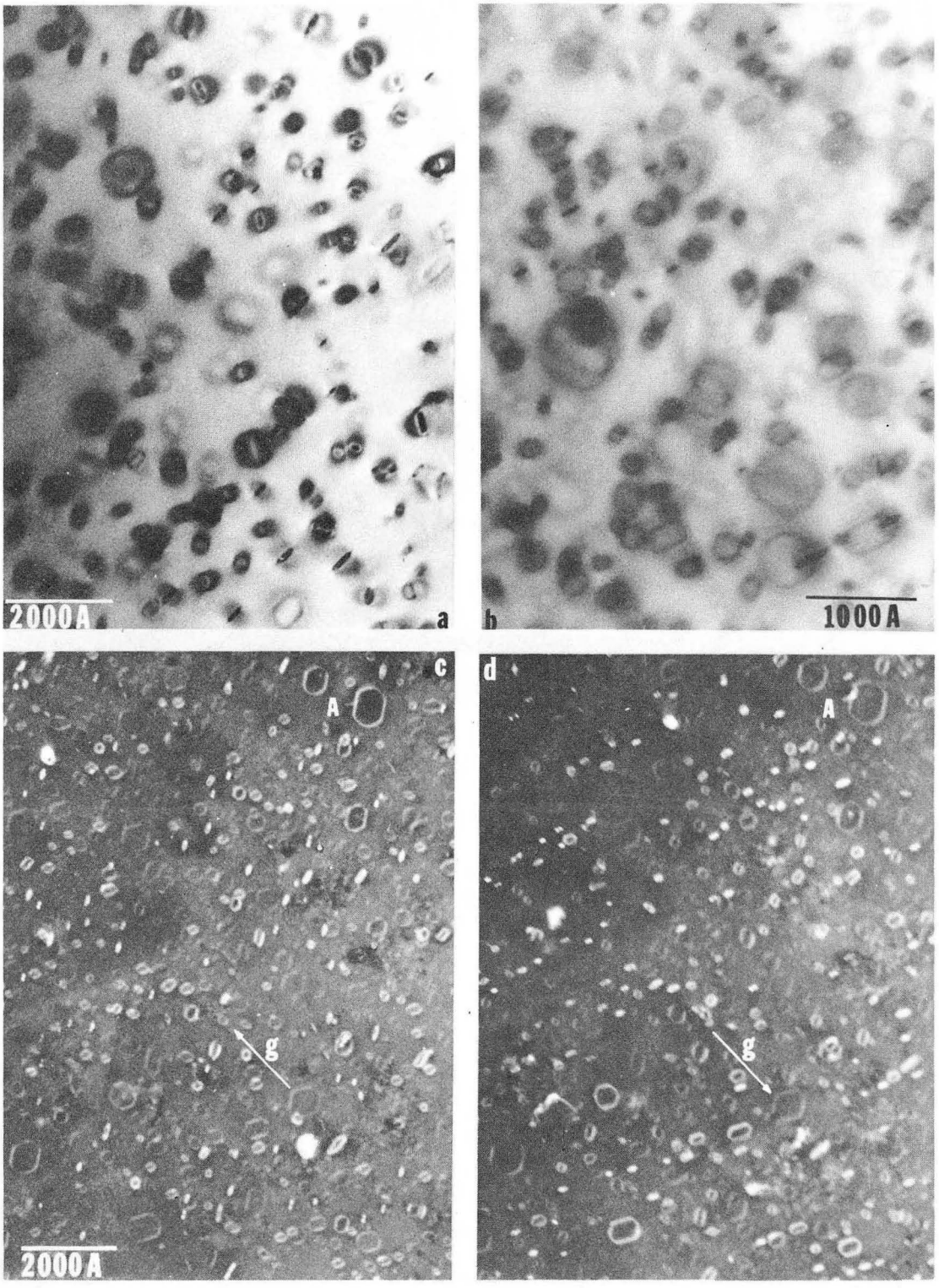


XBB 7410-7190

Fig. 5

*TECHNICAL INFORMATION DIVISION*
*LAWRENCE BERKELEY LABORATORY*
*UNIVERSITY OF CALIFORNIA*
*BERKELEY, CALIFORNIA 94720*